Catalpol attenuates lipopolysaccharide-induced inflammatory responses in BV2 microglia through inhibiting the TLR4-mediated NF-κB pathway

Yung Hyun Choi[1,2]

[1] *Department of Biochemistry, Dong-eui University College of Korean Medicine, 52-57, Yangjeong-ro, Busanjin, Busan 47227, Republic of Korea*

[2] *Anti-Aging Research Center, Dong-eui University, 176 Eomgwangno Busanjin-gu, Busan 47227, Republic of Korea*

Abstract. Catalpol, an iridoid glucoside mainly found in the root of *Rehmannia glutinosa* Libosch, is known to possess various pharmacological effects. Here, we investigated its inhibitory potential against inflammatory responses in lipopolysaccharide (LPS)-stimulated BV2 microglia. Our results showed that catalpol significantly suppressed LPS-induced secretion of pro-inflammatory mediators, including nitric oxide (NO) and prostaglandin E_2. Consistent with these results, catalpol downregulated LPS-stimulated expression of their regulatory enzymes, such as inducible NO synthase and cyclooxygenase-2. Catalpol also inhibited LPS-induced production and expression of pro-inflammatory cytokines, such as tumor necrosis factor-α and interleukin-1β. Additionally, catalpol suppressed the nuclear factor-kappa B (NF-κB) signaling pathway by disrupting the phosphorylation and degradation of inhibitor of κB-α and blocking the nuclear translocation of NF-κB p65. Moreover, catalpol inhibited LPS-induced expression of toll-like receptor 4 (TLR4) and myeloid differentiation factor 88, which was related to suppression of the binding of LPS with TLR4 on the cell surface. Furthermore, catalpol markedly reduced LPS-induced generation of reactive oxygen species (ROS). Collectively, these results suggest that catalpol can repress LPS-mediated inflammatory action in BV2 microglia through inactivating NF-κB signaling by antagonizing TLR4 and eliminating ROS, indicating that catalpol can have potential benefits by inhibiting the onset and/or treatment of inflammatory diseases.

Key words: Catalpol — Anti-inflammation — NF-κB — TLR4 — ROS

Introduction

Glial cells, including microglia and astrocytes, are the central nervous system (CNS) immune cells that play a critical role in the development and maintenance of the brain. However, these cells dysfunction due to hyperactivity in response to inflammatory signals is closely related to the onset and progression of various neurodegenerative diseases by damaging brain nerve cells (Tremblay et al. 2011; Gomez-Nicola and Perry 2015). Toll-like receptors (TLRs) among the various receptors that stimulate inflammatory signaling belong to the family of Toll homologous proteins, which functions as a receptor for recognition of pathogen-associated immune responses. Among bacterial endotoxins, lipopolysaccharides (LPS), present in the outer membrane of gram-negative bacteria, can induce excessive activation of glial cells through binding to TLR4, which was coupled with increased expression of TLR4 (Glass et al. 2010; Cherry et al. 2014). TLR4 ultimately activates a variety of downstream signaling pathways, including the nuclear factor-kappa B (NF-κB) signaling pathway, leading to elevated secretion of pro-inflammatory mediators and cytokines (Li and Verma 2002; Kopitar-Jerala, 2015; Lee et al. 2017). Therefore, antagonists to TLR4 can counteract the pro-inflammatory downstream signaling pathway by inhibiting different target gene expression and cellular responses. In addition, over-activated microglial cells stimulated by LPS can induce oxidative stress by increasing the generation of reactive oxygen species (ROS); this further aggravates the inflammatory response (von Bernhardi et al.

Correspondence to: Yung Hyun Choi, Department of Biochemistry, Dong-eui University College of Korean Medicine, Busan 47227, Republic of Korea
E-mail: choiyh@deu.ac.kr

2015; Daulatzai 2016). These observations suggest that blocking excessive activation of microglia is an important tool to delay the induction and progression of several brain diseases.

Rehmanniae Radix, the root of *Rehmannia glutinosa* Libosch, belongs to the Scrophulariaceae family, which has long been used for the prevention and treatment of various diseases in Korea and other Asian countries (Zhang et al. 2008; Matsumoto and Sekimizu 2016; Liu et al. 2017a). Catalpol is one of the iridoid glycoside compounds purified from Rehmanniae Radix. It is known to have several remarkable pharmacological effects, such as anti-asthma (Chen et al. 2017), anti-diabetic (Bao et al. 2016; Zhu et al. 2016), hypoglycemic (Li et al. 2014), and antitumor (Jin et al. 2015; Liu et al. 2017b; Wang and Zhan-Sheng 2018) properties. It has also been reported that catalpol acts as a neuroprotective agent for ischemic injury and neurodegenerative diseases (Tian et al. 2006; Zhang et al. 2007; Zheng et al. 2017). In addition, its antioxidant effect can be achieved by blocking ROS production (Jiang et al. 2008; Bi et al. 2013; Cai et al. 2016). As previously reported, catalpol has also shown potent anti-inflammatory effects in a variety of experimental models using LPS and inflammatory cytokines (Tian et al. 2006; Zhang et al. 2009, 2016; Bi et al. 2013; Fu et al. 2014; Zhou et al. 2015), which were found to be related to inhibition of NF-κB signaling activity (Zhang et al. 2009, 2017; Choi et al. 2013; Xiao et al. 2014; Zhou et al. 2015). Although it has been suggested that TLR4 may be involved in the anti-inflammatory effects of catalpol (Bi et al. 2013; Fu et al. 2014; Zhang et al. 2016), the precise role of TLR4 in relation to the protective effects of catalpol has not yet been established. Moreover, studies on the microglial cell model have not been performed properly. Therefore, the objective of this study was to examine the anti-inflammatory potency of catalpol and determine the effect of catalpol on activation of the TLR4 signaling pathway in BV2 microglia stimulated by LPS.

Materials and Methods

Materials and reagents

The cell culture medium, Dulbecco's modified Eagle medium (DMEM), fetal bovine serum (FBS), and other tissue culture reagents were purchased from WelGENE Inc. (Daegu, Republic of Korea). Catalpol, LPS, Griess reagent, bovine serum albumin (BSA), dimethyl sulfoxide (DMSO), 3-(4,5-dimethylthiazol-2-yl)-2,5-diphenyltetrazolium bromide (MTT), 4',6-diamidino-2-phenylindole (DAPI) and 5,6-carboxy-2',7'-dichlorofluorescin diacetate (DCF-DA) were purchased from Sigma-Aldrich Chemical Co. (St. Louis, MO, USA). The enzyme-linked immunosorbent assay (ELISA) kits for prostaglandin E_2 (PGE_2), tumor necrosis factor (TNF)-α, and interleukin (IL)-1β were obtained from R&D Systems (Minneapolis, MN, USA). TRIzol reagent,

inducible nitric oxide (NO) synthase, cyclooxygenase-2 (COX-2), TNF-α, IL-1β and glyceraldehyde-3-phosphate dehydrogenase (GAPDH) oligonucleotide primers were purchased from Bioneer (Seoul, Republic of Korea). NE-PER Nuclear and Cytoplasmic Extraction Reagents kit and polyvinylidene difluoride (PVDF) membranes were purchased from Pierce Biotechnology (Rockford, IL, USA) and Schleicher and Schuell (Keene, NH, USA), respectively. Primary antibodies and appropriate horseradish-peroxidase (HRP)-conjugated secondary antibodies used for Western blot analysis were purchased from Santa Cruz Biotechnology Inc. (Santa Cruz, CA, USA) and Cell Signaling Technology (Beverly, MA, USA). An enhanced chemiluminescence (ECL) detection kit was purchased from Amersham Corp. (Arlington Heights, IL, USA). Fluorescein-conjugated anti-rat IgG and Alexa Fluor (AF) 488-conjugated LPS were obtained from Life Technologies (Carlsbad, CA, USA) and Molecular Probes Inc. (Leiden, Netherlands), respectively. All other chemicals were obtained from Sigma-Aldrich Chemical Co. unless indicated otherwise.

Cell culture and LPS stimulation

BV2 microglia were maintained in DMEM containing 10% FBS, L-glutamine (2 mM), penicillin (100 U/ml), and streptomycin (100 μg/ml) at 37°C in a humidified atmosphere with 5% CO_2 and 95% air. Catalpol was dissolved in DMSO and adjusted to the final concentration using complete culture medium. To stimulate BV2 cells, the medium was replaced with fresh DMEM and 100 ng/ml LPS was added in the presence or absence of catalpol for the indicated time periods.

Assessment of cell viability

To determine cell viability, BV2 cells were seeded into 96-well plates at a density of 1×10^4 cells *per* well. After 24 h of incubation, cells were treated with various concentrations of catalpol or pretreated with different concentrations of catalpol for 1 h before LPS (100 ng/ml) treatment for 24 h. Afterward, the medium was removed and 0.5 mg/ml MTT solution was added to each well. After incubation at 37°C for 3 h, the supernatant was then replaced with DMSO to dissolve blue formazan crystals in each well. After 10 min of incubation at 37°C, the optical density was measured at a wavelength of 540 nm on an ELISA microplate reader (Dynatech Laboratories, Chantilly, VA, USA). The optical density of formazan formed in control (untreated) cells was taken as 100% viability.

Measurement of pro-inflammatory mediators and cytokines production

Levels of NO production were indirectly determined by measuring stable NO catabolite nitrite in a medium by

Griess reaction. Briefly, the conditioned medium (100 μl) was mixed with the same volume of Griess reagent and incubated at room temperature for 10 min. The optical density at 540 nm was then measured on an ELISA microplate reader and the concentration of nitrite was calculated according to a standard curve generated from known concentrations of sodium nitrite. Levels of PGE_2, TNF-α and IL-1β in the culture medium were measured using commercial ELISA kits, according to the manufacturer's instructions, as described previously (Choi et al. 2017).

RNA isolation and reverse transcriptase-polymerase chain reaction (RT-PCR)

BV2 cells were pretreated with various concentrations of catalpol for 1 h, followed by treatment with 100 ng/ml LPS for 24 h. Total RNA from isolated cells was prepared using a TRIzol reagent, following the manufacturer's instructions, and quantified. For mRNA expression analysis, cDNA was synthesized from 1 μg of total RNA using AccuPower® RT PreMix (Bioneer, Daejeon, Korea) containing moloney murine leukemia virus reverse transcriptase. The RT-generated cDNA was amplified using selected primers, under the following conditions: 10 min at 95°C, followed by 40 cycles of 15 s at 95°C and 1 min at 60°C. GAPDH was used as an internal control.

Protein isolation and Western blot analysis

Cells were collected, and cellular proteins were prepared, as described previously (Park et al. 2017). Cytosolic and nuclear proteins were separated using a commercial kit according to the manufacturer's protocol. For Western blotting, equal amounts of protein samples were resolved by sodium dodecyl sulfate-polyacrylamide gel electrophoresis and transferred onto PVDF membranes. Subsequently, the membranes were blocked with 5% non-fat dry milk/Tris-buffered saline containing 0.1% Triton X-100 (TBST) for 1 h and incubated with the appropriate antibodies at 4°C overnight. After washing membranes with TBST, they were incubated with the appropriate HRP-conjugated secondary antibodies for 2 h at room temperature. Protein bands were visualized using an ECL kit according to the manufacturer's instructions.

Immunofluorescence staining for nuclear translocation of NF-κB and formation of LPS/TLR4 complexes

After cells were pretreated with or without 500 μM catalpol for 1 h, they were treated with 100 ng/ml LPS. The cells were then fixed in 3.7% paraformaldehyde for 15 min, permeabilized with 0.2% Triton X-100 in phosphate-buffered saline (PBS) for 15 min, and blocked with PBS containing 5% BSA. The cells were then stained with primary antibody against NF-κB p65 at 4°C overnight followed by incubation with a fluorescein-conjugated anti-rat IgG in the dark at 37°C for 40 min. In addition, these cells were treated with AF 488-conjugated LPS (100 ng/ml) for 30 min in the presence or absence of catalpol to analyze the formation of LPS/TLR4 complexes. Fixed cells were also stained with anti-TLR4 antibody at 4°C for 90 min and then incubated with secondary antibody conjugated with Alexa Fluor 594 at room temperature for 1 h. Nuclei were sequentially stained with DAPI solution (2.5 μg/ml). Slides were mounted and fluorescence images were captured by fluorescence microscopy (Carl Zeiss, Oberkochen, Germany).

Measurement of TLR4 expression on cell surface

To investigate the effect of catalpol on TLR4 expression on the cell surface, AF-LPS was used to treat BV2 cells pretreated with or without catalpol for 1 h. After treatment, cells were washed twice with PBS, harvested with 0.005% ethylenediaminetetraacetic acid, and then analyzed by flow cytometry. Alexa 488 was excited using 488 argon ion laser lines and detected on channel FL1 using a 530 nm emission filter. Fluorescence emission of samples was recorded by flow cytometry (Becton Dickinson, San Jose, CA, USA) as previously described (Lee et al. 2012).

Detection of intracellular ROS levels

Production of intracellular ROS was monitored using DCF-DA. In short, cells were treated with 500 μM catalpol for 1 h or pretreated with 500 μM catalpol for 1 h followed by culture for 1 h in the presence or absence of 100 ng/ml LPS. These cells were harvested and stained with 10 μM DCF-DA in the dark at 37°C for 15 min. After rinsing twice with PBS, cells were immediately analyzed by flow cytometry with an excitation wavelength of 480 nm and an emission wavelength of 525 nm. To observe the degree of ROS production by fluorescence microscopic observation, cells attached to glass coverslips were stimulated with or without 100 ng/ml LPS after 500 μM catalpol treatment for 1 h. These cells were stained with DCF-DA, washed twice with PBS, and fixed with 4% paraformaldehyde (pH 7.4) for 20 min, after which the fixed cells were analyzed by fluorescence microscopy.

Statistical analysis

Results are presented as the mean ± the standard deviation (SD). Statistical significance was assessed using Statistical Package for the Social Sciences (SPSS) software (version 18.0) to identify significant differences based on one-way analysis of variance (ANOVA) followed by Dunn's post-hoc tests. Statistical significance was considered at *p* value < 0.05.

Results

Catalpol suppresses LPS-induced NO and PGE_2 production in BV2 microglial cells

To examine the inhibitory effect of catalpol on LPS-induced production of pro-inflammatory mediators, including NO and PGE_2, BV2 cells were pretreated with different concentrations of catalpol (0, 100, 250 or 500 μM) for 1 h and then stimulated with 100 ng/ml LPS for another 24 h. Levels of NO and PGE_2 in culture supernatants were determined by Griess reaction assay and ELISA, respectively. As shown in Figures 1A and B, stimulation with LPS alone markedly increased NO and PGE_2 production in comparison with no

stimulation with LPS ($p < 0.05$ vs. control; about 12-fold and 15-fold, respectively). Conversely, catalpol significantly suppressed LPS-induced secretion of NO and PGE_2 in BV2 cells in a concentration-dependent manner. Significant repression was observed with 100 μM of catalpol ($p < 0.05$ vs. LPS).

Catalpol attenuates LPS-induced iNOS and COX-2 expression in BV2 microglial cells

We next investigated whether the inhibitory effects of catalpol on NO and PGE_2 production were related to regulation of the expression of their synthesis enzymes, such as iNOS and COX-2. The results of RT-PCR and immunoblotting demonstrated that catalpol concentration-dependently
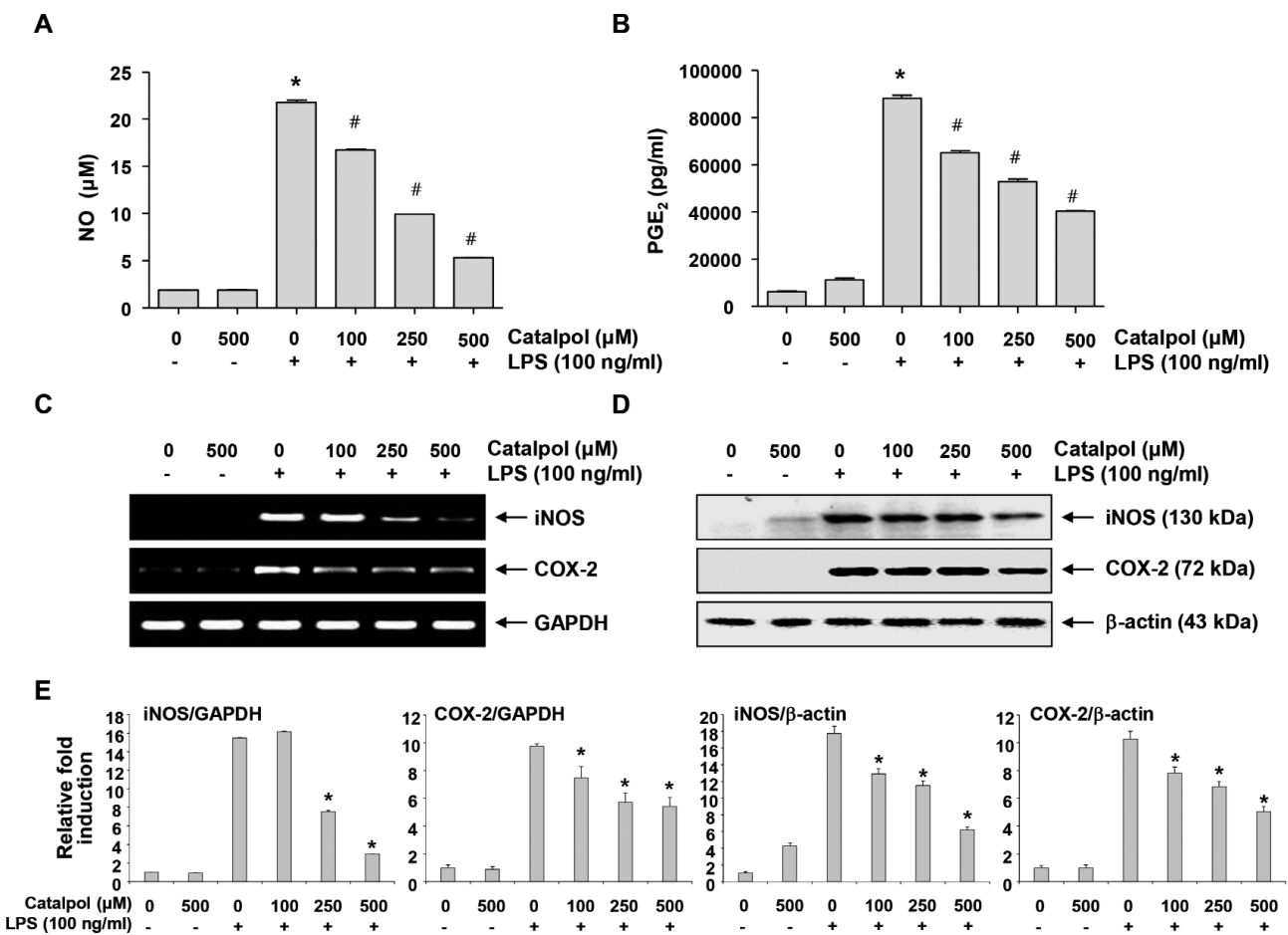

Figure 1. Suppression of LPS-induced production NO and PGE_2 and expressions of iNOS and COX-2 by catalpol in BV2 microglial cells. Cells were pretreated with the indicated concentrations of catalpol for 1 h prior to incubation with 100 ng/ml LPS for 24 h. The levels of NO (**A**) and PGE_2 (**B**) in culture media were measured by Griess assay and a commercial ELISA kit, respectively. Each value indicates the mean ± SD as a representative result obtained from three independent experiments (* $p < 0.05$ compared to control; # $p < 0.05$ compared to cells cultured with 100 ng/ml LPS). The mRNA (**C**) and protein (**D**) levels of iNOS and COX-2 were determined by RT-PCR and Western blot analysis, respectively. GAPDH and β-actin were used as internal controls for the RT-PCR and Western blot assay, respectively. **E.** Bands were quantified using ImageJ and normalized to GAPDH and β-actin, and the ratio was determined. Data are expressed as mean ± SD. All experiments were repeated three times (* $p < 0.05$ compared with the LPS group).

inhibited expression levels of iNOS and COX-2 mRNA and protein in LPS-stimulated BV2 cells ($p < 0.05$ *vs*. LPS). This finding indicates that catalpol can suppress NO and PGE_2 production by reducing the expression of their encoding genes at the transcriptional levels.

Catalpol reduces the production and expression of pro-inflammatory cytokines in LPS-stimulated BV2 microglial cells

The effect of catalpol on the production of pro-inflammatory cytokines, including TNF-α and IL-1β, in LPS-stimulated BV2 cells was determined. According to our ELISA results (Figures 2A and B), the production of the two cytokines was significantly increased in the culture medium of LPS-stimulated BV2 cells ($p < 0.05$ *vs*. control) but decreased in the presence of catalpol in a concentration-dependent manner ($p < 0.05$ *vs*. LPS). In addition, suppression of TNF-α and IL-1β production by catalpol was associated with inhibition of the expression of these genes (Figures 2C and D), suggesting that catalpol LJGP prevented pro-inflammatory cytokine production through suppression of their gene expression in LPS-stimulated BV2 microglia.

Effect of catalpol on cell viability in BV2 microglial cells

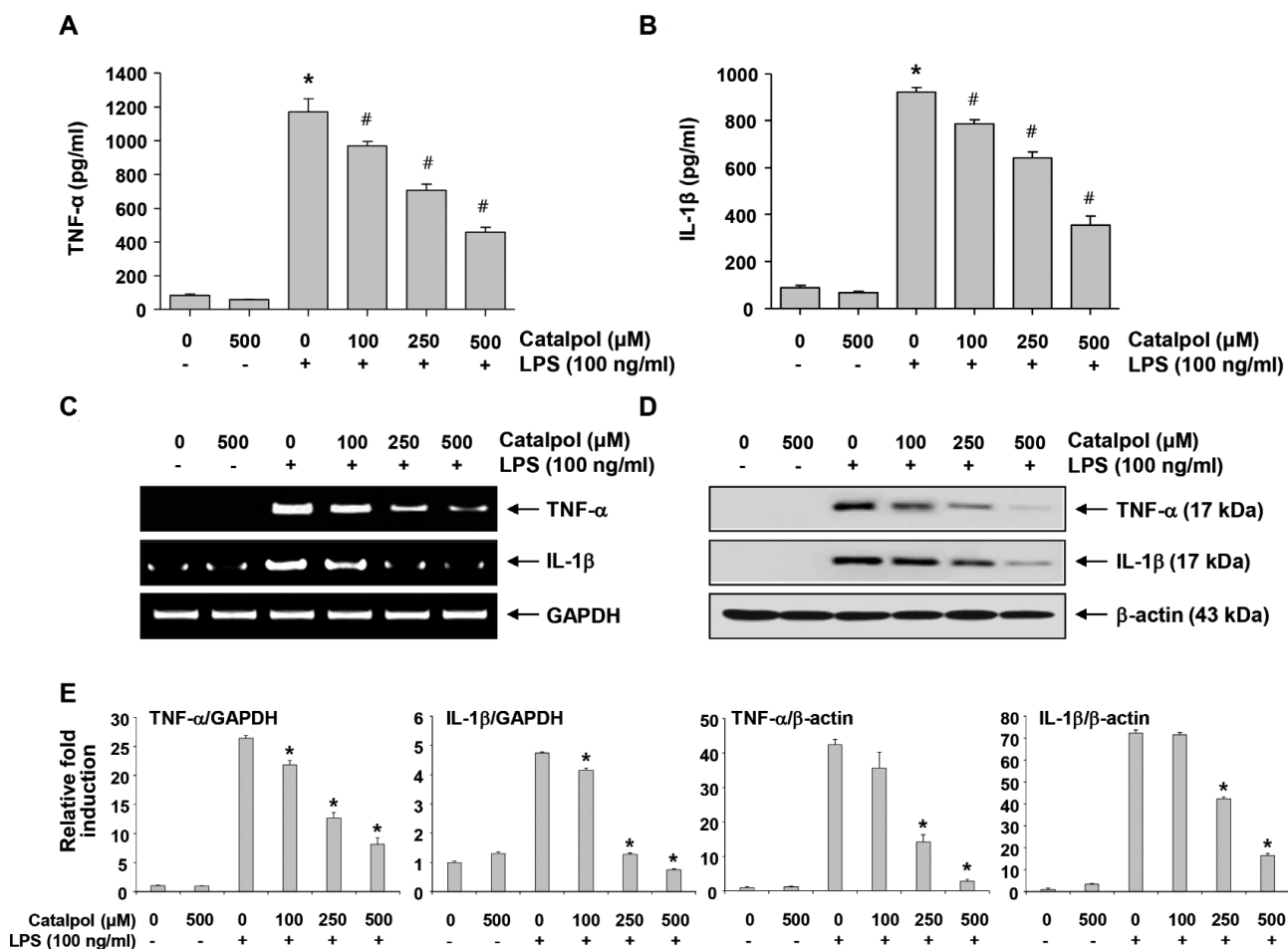An MTT assay was performed to investigate whether the inhibitory effect of catalpol on production of pro-

Figure 2. Inhibition of LPS-induced production and expression of TNF-α and IL-1β by catalpol in BV2 microglial cells. BV2 cells were pretreated with various concentrations of catalpol for 1 h followed by treatment with 100 ng/ml LPS for 24 h. The levels of TNF-α (**A**) and IL-1β (**B**) present in the supernatants were measured using the corresponding ELISA kits. Each value indicates the mean ± SD as a representative result obtained from three independent experiments (* $p < 0.05$ compared to control; # $p < 0.05$ compared to cells cultured with 100 ng/ml LPS). The mRNA (**C**) and protein (**D**) levels of TNF-α and IL-1β were determined by RT-PCR and Western blot analysis, respectively. GAPDH and β-actin were used as internal controls for the RT-PCR and Western blot assay, respectively. **E.** Bands were quantified using ImageJ and normalized to GAPDH and β-actin, and the ratio was determined. Data are expressed as mean ± SD. All experiments were repeated three times (* $p < 0.05$ compared with the LPS group).
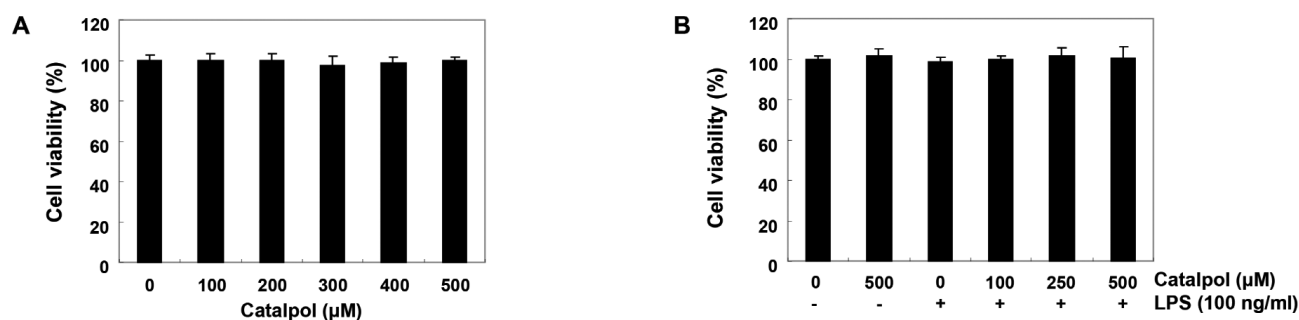
Figure 3. The effects of catalpol and LPS on the viability of BV2 microglial cells. Cells were treated with various concentrations of catalpol for 24 h (**A**) or pre-treated with the indicated concentrations of catalpol for 1 h prior to treatment with 100 ng/ml LPS for 24 h (**B**). Cell viability was assessed by MTT assay. Results are expressed as the percentage of surviving cells over control cells (no addition of catalpol or LPS). Values represent the mean ± SD of three independent experiments.

inflammatory mediators and cytokines was due to the cytotoxicity of catalpol. Figure 3 showed that the survival rate of BV2 cells was not significantly affected by treatment with catalpol alone at a concentration of up to 500 μM for 24 h, even in the presence of 100 ng/ml LPS. LPS markedly induced morphological changes of BV2 microglia after treatment with LPS, which was consequently improved by the treatment with catalpol (data not shown). Therefore,
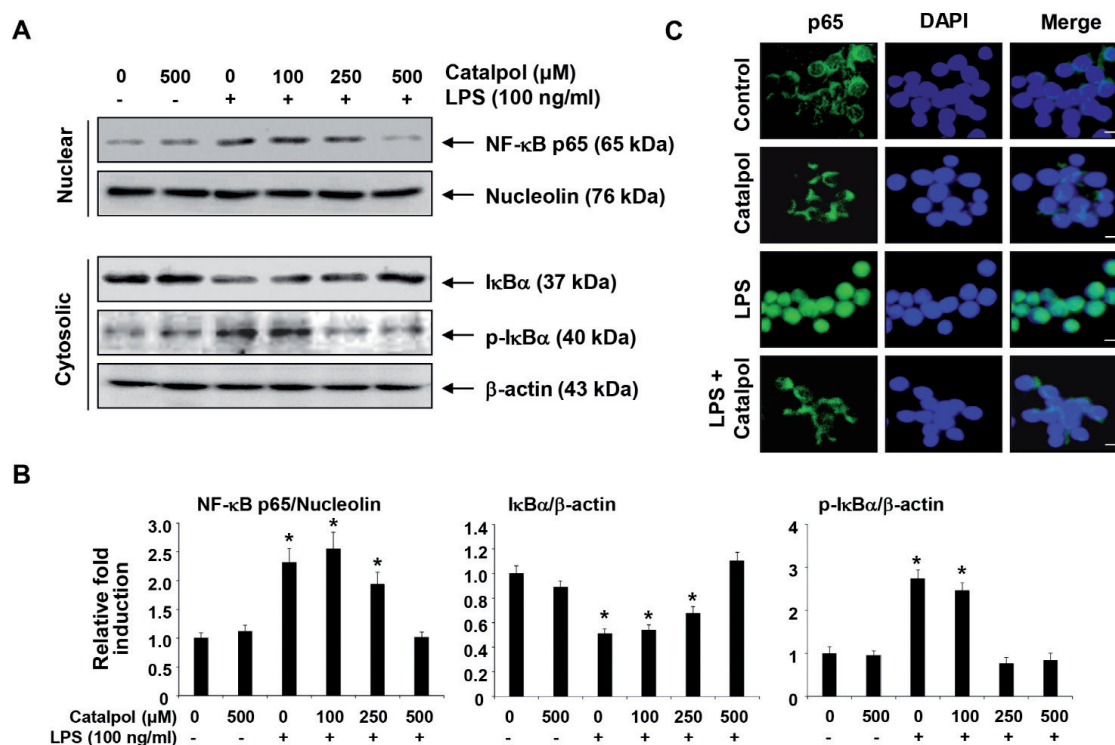

Figure 4. Inhibition of NF-κB nuclear translocation by catalpol in LPS-stimulated BV2 microglial cells. **A.** Cells were pre-treated with the indicated concentrations of catalpol for 1 h before treatment with 100 ng/ml LPS for 1 h. Nuclear and cytosolic proteins were prepared for Western blot analysis using anti-NF-κB p65, anti-p-IκBα, and anti-IκBα antibodies with an ECL detection system. Nucleolin and β-actin were used as internal controls for nuclear and cytosolic fractions, respectively. **B.** Bands were quantified using ImageJ and normalized to nucleolin and β-actin, and the ratio was determined. Data are expressed as mean ± SD. All experiments were repeated three times (* $p < 0.05$ compared to control). **C.** Cells were pre-treated with 500 μM catalpol for 1 h before treatment with 100 ng/ml LPS for 1 h. The localization of NF-κB p65 was visualized by fluorescence microscopy after immunofluorescence staining with an anti-NF-κB p65 antibody (green). These cells were also stained with DAPI to visualize the nuclei (blue). Results are representative of three independent experiments. Scale bars, 10 μm.

the anti-inflammatory effect by catalpol was not due to the cytotoxicity of catalpol, but to catalpol itself.

Catalpol alleviates LPS-induced NF-κB nuclear translocation and inhibitor of κB-α (IκBα) degradation in BV2 microglial cells

Subsequently, we determined whether catalpol could attenuate LPS-induced activation of NF-κB in BV2 cells. Immunoblotting data using cytoplasmic and nuclear extracts showed

that catalpol pretreatment inhibited nuclear accumulation of the NF-κB p65 subunit associated with attenuation of phosphorylation and degradation of IκBα in LPS-stimulated BV2 cells in a concentration-dependent manner (Figure 4A). Consistent with these results, immunocytochemical analysis indicated that the fluorescence intensity of NF-κB p65 in the nucleus was increased in LPS-stimulated cells. However, LPS-mediated nuclear translocation of NF-κB was considerably blocked by pretreatment with 500 μM catalpol (Figure 4B), implying that catalpol could attenuate
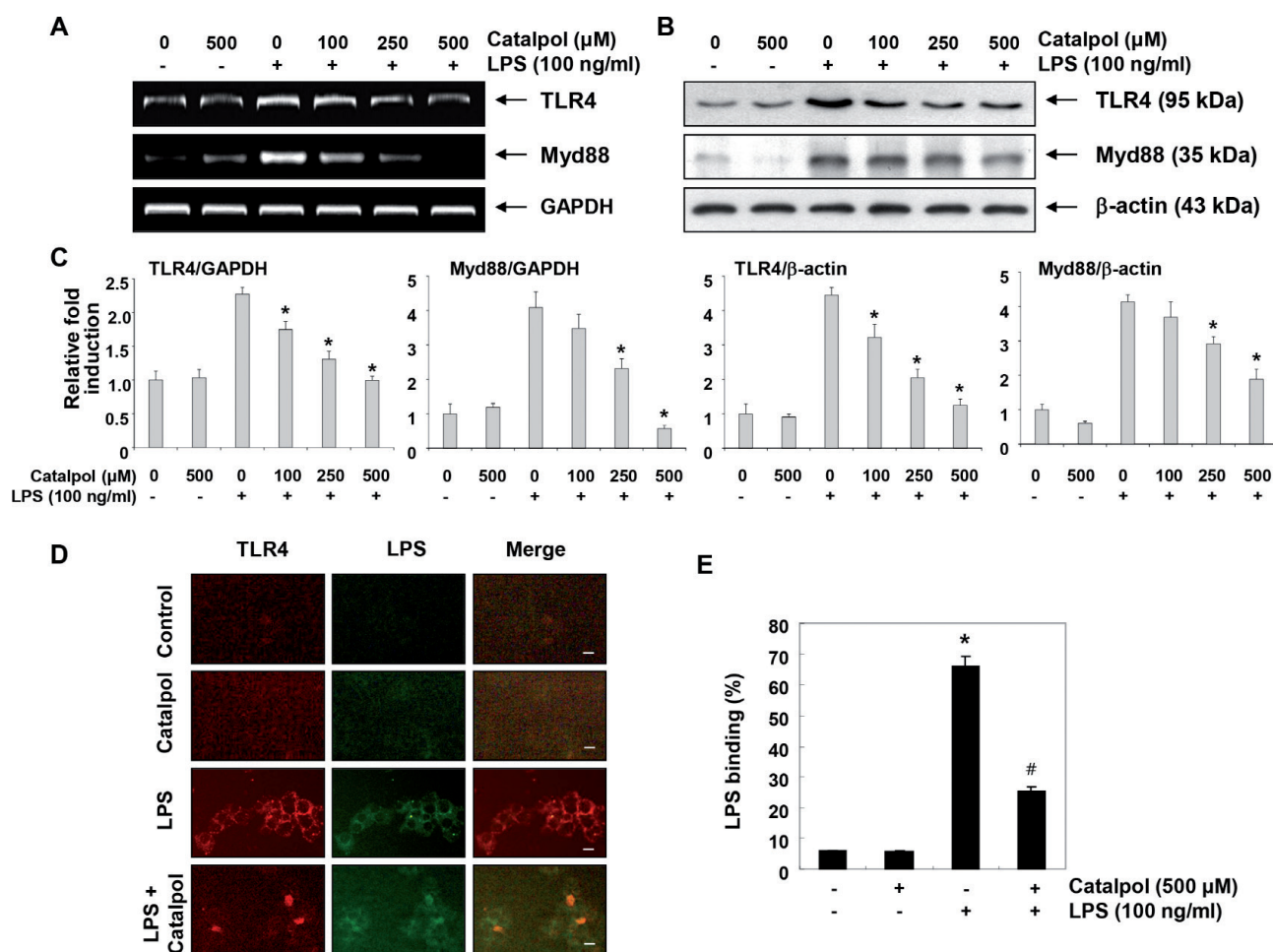

Figure 5. Attenuation of LPS-induced expression of TLR4 and Myd88, and interaction between LPS and TLR4 by catalpol in BV2 microglial cells. **A, B.** Cells were pretreated with the indicated concentrations of catalpol for 1 h prior to 100 ng/ml LPS treatment for 6 h. The mRNA (A) and protein (B) levels of TLR4 and Myd88 were determined by RT-PCR and Western blot analysis, respectively. GAPDH and β-actin were used as internal controls for the RT-PCR and Western blot assay, respectively. **C.** Bands were quantified using ImageJ and normalized to GAPDH and β-actin, and the ratio was determined. Data are expressed as mean ± SD. All experiments were repeated three times (* $p < 0.05$ compared with the LPS group). **D.** Cells were incubated with 100 ng/ml AF-LPS for 1 h in the absence or presence of 500 μM catalpol. After 6 h of incubation, the distribution of AF-LPS and TLR4 was detected by fluorescence microscopy. Experiments were repeated three times with similar results. Scale bars, 10 μm. **E.** After treatment with 100 ng/ml AF-LPS for 1 h in the absence or presence of 500 μM catalpol, LPS binding on the surface of BV2 cells was measured by flow cytometry. Data are presented as the mean ± SD as representative results obtained from three independent experiments (* $p < 0.05$ compared to control; # $p < 0.05$ compared to cells cultured with 100 ng/ml AF-LPS).

LPS-induced activation of NF-κB. Therefore, these results indicate that the inactivation of NF-κB by catalpol may be a mechanism responsible for suppression of NO, PGE$_2$ and pro-inflammatory cytokines in BV2 cells.

Catalpol inhibits LPS-induced TLR4 and Myd88 expression, and interaction between LPS and TLR4 in BV2 microglial cells

To determine whether the anti-inflammatory effect of catalpol was related to blocking the TLR4 signaling pathway, the effects of LPS and catalpol on expression of TLR4 and myeloid differentiation factor 88 (Myd88) were investigated. Results of immunoblotting revealed that levels of the TLR4 and Myd88 proteins were markedly increased by LPS treatment; however, when catalpol was pretreated, LPS-induced expression of these proteins was markedly inhibited (Figure 5A). We further assessed whether catalpol could inhibit the interaction between LPS and TLR4 on an LPS-treated BV2 cell surface. As shown in Figures 5B–D, the increased fluorescence of LPS and TLR4 was observed outside the cell membrane in LPS-treated BV2 cells. However, the fluorescence intensity of TLR4 and the binding activity of LPS on the cell surface were significantly attenuated in BV2 cells treated with LPS in the presence of catalpol ($p < 0.05$ *vs.* LPS).

Catalpol diminishes LPS-induced ROS generation in BV2 microglial cells

To investigate the antioxidant potential of catalpol, the effect of catalpol on LPS-induced ROS production was examined. Flow cytometry results showed that the level of ROS was gradually increased after treatment with LPS ($p < 0.05$ *vs.* control), peaking at 1 h. It was decreased thereafter (data not shown). However, treatment with catalpol alone did not induce ROS generation, and pretreatment with catalpol effectively attenuated the level of ROS released by LPS ($p < 0.05$ *vs.* LPS; Figure 6A). The inhibitory effect of catalpol on ROS production was similarly observed in experiments using fluorescence microscopy (Figure 6B and C). In N-acetyl cysteine (NAC, 10 mM)-pretreated cells used as a positive control, the production of ROS stimulated by LPS was significantly blocked ($p < 0.05$ *vs.* LPS), indicating that catalpol had a strong ROS scavenging effect.

Discussion

Expression of iNOS and COX-2 in glial cells is increased in inflammatory conditions leading to the increased synthesis of
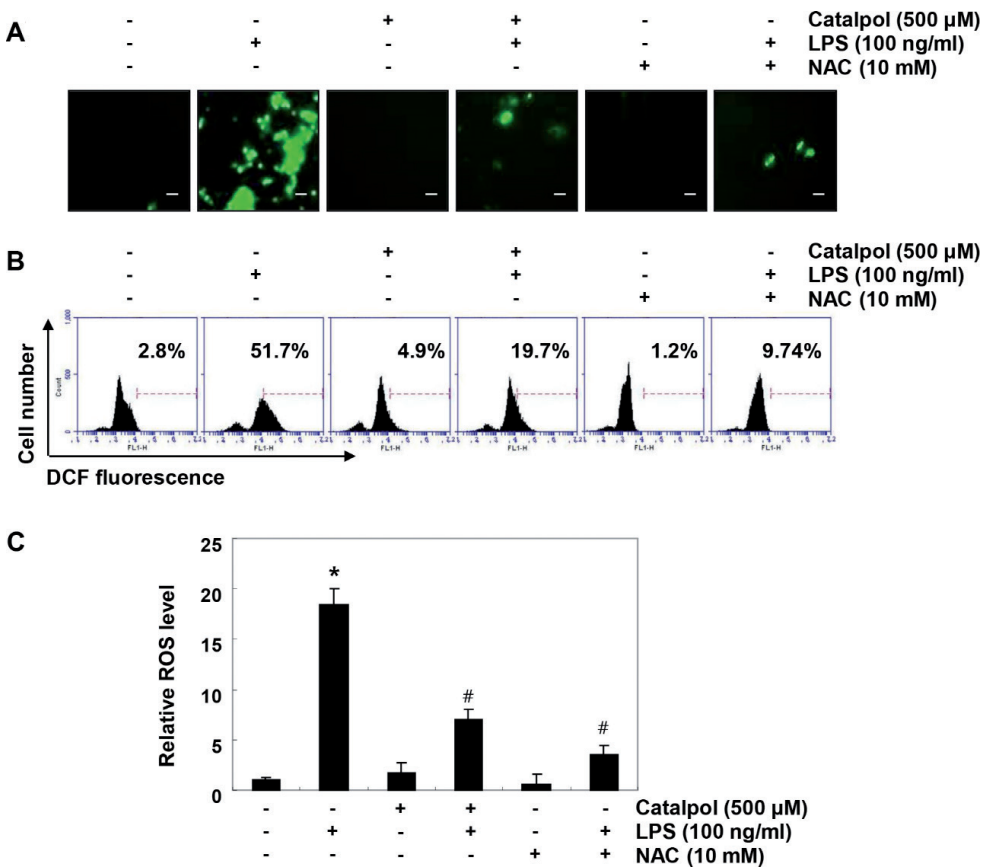

Figure 6. Inhibition of LPS-induced ROS generation by catalpol in BV2 microglial cells. Cells were pretreated with 500 μM catalpol or 10 mM NAC for 1 h followed by stimulation with or without 100 ng/ml LPS for 1 h. **A.** After staining with DCF-DA, images were obtained by fluorescence microscopy (original magnification, ×200). Scale bars, 10 μm. These images are representative of at least three independent experiments. **B.** Cells were incubated with DCF-DA and DCF fluorescence was measured by flow cytometry. These images are representative of at least three independent experiments. **C.** Each value indicates the mean ± SD as a representative result obtained from three independent experiments (* $p < 0.05$ compared to control; # $p < 0.05$ compared to cells cultured with 100 ng/ml LPS).

NO and PGE_2. Such regulation of NO and PGE_2 production during neuroinflammation plays an important role in the regulation of inflammatory balance by glial cells (Tremblay et al. 2011; Gomez-Nicola and Perry 2015). Results of the current study showed that catalpol inhibited LPS-induced inflammatory signaling in BV2 microglia, a brain microglial cell line. Similar to results of previous studies (Tian et al. 2006; Bi et al. 2013), catalpol could significantly inhibit the increased production of NO and PGE_2 by LPS in the absence of cytotoxicity, which was associated with suppression of iNOS and COX-2 mRNA and protein expression. We also found that catalpol reduced the release of inflammatory cytokines such as TNF-α and IL-1β by blocking their expression in LPS-stimulated BV2 cells, very similar to the results of previous studies (Tian et al. 2006; Fu et al. 2014; Zhang et al. 2017). These results suggest that catalpol may attenuate inflammatory response by inhibiting the expression of genes that regulate the production of pro-inflammatory factors.

NF-κB is a key transcription factor that increases the expression of pro-inflammatory enzymes and cytokines only if it has migrated to the nucleus. In un-activated cells, NF-κB is usually located in the cytoplasm in association with IκBα, which suppresses the activation signal upon translocalization to the nucleus. When IκBα is phosphorylated and degraded, a key step in the activation of NF-κB, NF-κB is isolated and translocated to the nucleus (Li and Verma 2002; Kopitar-Jerala 2015; Lee et al. 2017). Thus, we determined whether catalpol could inhibit LPS-induced degradation of IκBα and nuclear translocation of NF-κB. Our results indicated that catalpol could effectively block nuclear expression of NF-κB (p65), and the phosphorylation and degradation of IκBα in LPS-treated BV2 microglial cells. These results suggest that catalpol can reduce the expression and production of pro-inflammatory mediators and cytokines by inhibiting the NF-κB pathway in LPS-stimulated BV2 microglia. This is in line with previous findings that catalpol inhibited the activation of NF-κB in LPS-induced acute lung injury and acute systemic inflammation, and LPS-mediated inflammatory responses in astrocytic primary cultures (Zhang et al. 2009; Bi et al. 2013; Fu et al. 2014).

Immune cells, including microglia, can recognize pathogen-associated molecular patterns through TLR pattern recognition receptors expressed on the cell surface. Among the various TLRs, TLR4 is known to recruit adapter molecules, including MyD88, LPS-binding protein (LPB), myeloid differentiation protein 2 (MD2), and differentiation cluster co-receptor when immune cells are activated by LPS (Tremblay et al. 2011; Gomez-Nicola and Perry 2015). Upon activation of TLR4 by LPS, a TLR4-MyD88-mediated signal can induce the activation of mitogen-activated protein kinases (MAPKs), which eventually promotes the activation of NF-κB signaling and ultimately produces pro-inflammatory mediators and cytokines (Glass et al. 2010;

Cherry et al. 2014). In this study, we found that catalpol suppressed LPS-induced expression of TLR4 and MyD88. It also reduced the binding of TLR4 to LPS on the cell surface. This indicates that catalpol can inhibit the expression of pro-inflammatory enzymes and cytokines by blocking the TLR4 signaling pathway, the early stage of intracellular signaling in LPS-stimulated cells. This finding demonstrates that catalpol can attenuate the onset of the LPS-mediated intracellular signaling pathway by suppressing activation of NF-κB and inhibiting the binding of LPS to TLR4 in BV2 cells. According to the results of Fu et al. (2014), catalpol significantly inhibited expression of TLR4 and activation of NF-κB, and MAPKs in LPS-mediated acute lung injury. Bi et al. (2013) also reported that suppressive action of catalpol on inflammation was mediated *via* inhibiting TLR expression and NF-κB activation by LPS plus interferon (INF)-γ stimulation in primary cultured astrocytes. Thus, catalpol might be able to inhibit the NF-κB and MAPK signaling pathways by showing antagonistic effects on the binding of LPS to TLR4.

Oxidative stress (along with inflammatory stimuli) is another major cause of CNS damage. Low levels of ROS play an important role as signaling molecules that regulate the immune response to pathogens, but the overproduction of ROS contributes to neurotoxicity (von Bernhardi et al. 2015; Ohl et al. 2016; Fetisova et al. 2017). In many previous studies, inflammatory responses by LPS in microglia were directly related to increased ROS production, and inhibition of inflammatory response was reported to be associated with blocking ROS production (Fan et al. 2015; Iizumi et al. 2016; Garcia et al. 2017; Kim et al. 2017). TLR4 signaling-mediated generation of ROS by LPS accelerates inflammatory response by activating downstream signaling cascades containing NF-κB (Zeng et al. 2012; Wang et al. 2014; Slusarczyk et al. 2016). Therefore, inhibiting ROS production is an important strategy to suppress inflammatory responses and oxidative stress. From the perspective of inhibiting the production of ROS, our results are consistent with several previous studies. For example, the beneficial effects of catalpol on LPS-induced neurotoxicity in mesencephalic neuron-glia cultures and LPS plus IFN-γ-induced inflammatory response in astrocytes primary cultures are directly related to its antioxidant effects (Tian et al. 2006; Bi et al. 2013). In addition, the protective effect of catalpol on oxidative stress- and ischemia-induced damage in astrocytes and oligodendrocytes is associated with its blocking of ROS production (Bi et al. 2008, 2013; Li et al. 2008; Cai et al. 2016). These results are in line with results showing its antioxidant efficacy, observed in the present study, showing that catalpol can effectively block the production of excessive ROS induced by LPS. Although the inhibitory effect of catalpol on ROS production in the microglia model is reported in this study for the first time, additional studies
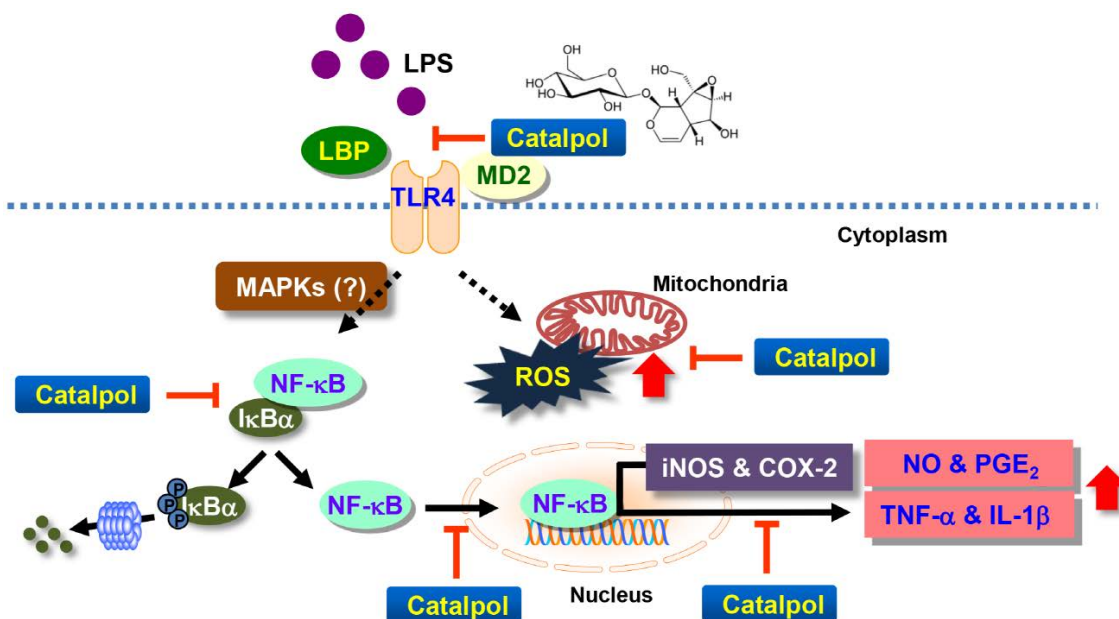
Figure 7. A schematic figure of possible signaling mechanisms of catalpol in the inhibition of LPS-induced inflammation response.

in primary cultures of microglia and astrocytes are needed to determine the direct linkage between ROS production blockade and anti-inflammatory efficacy.

In conclusion, the results obtained in this study demonstrated that catalpol had a potent anti-inflammatory effect on BV2 microglial cells. In LPS-stimulated BV2 cells, catalpol was able to reduce pro-inflammatory mediators and cytokine production, which was associated with decreased expression of their regulatory genes by suppressing NF-κB activity and ROS accumulation. Moreover, catalpol could block the aggregation of LPS to TLR4 on the cell surface, and interfering TLR4 signaling increased the anti-inflammatory potential of catalpol in BV2 microglia, suggesting the antagonistic effect of catalpol against TLR4, suggesting the antagonistic effect of catalpol against TLR4 (Figure 7). Although the results of the current study may provide a partial understanding of the mechanism involved in the anti-inflammatory effect of catalpol, further studies are needed to assess the mechanical role of catalpol in a variety of oxidative stresses and inflammatory mediated diseases.

Conflict of interest. The author has no conflict of interest to declare.

References

Bao Q, Shen X, Qian L, Gong C, Nie M, Dong Y (2016): Anti-diabetic activities of catalpol in db/db mice. Korean J. Physiol. Pharmacol. **20,** 153–160
https://doi.org/10.4196/kjpp.2016.20.2.153

Bi J, Jiang B, Liu JH, Lei C, Zhang XL, An LJ (2008): Protective effects of catalpol against H2O2-induced oxidative stress in astrocytes primary cultures. Neurosci. Lett. **442,** 224–227
https://doi.org/10.1016/j.neulet.2008.07.029

Bi J, Jiang B, Zorn A, Zhao RG, Liu P, An LJ (2013): Catalpol inhibits LPS plus IFN-γ-induced inflammatory response in astrocytes primary cultures. Toxicol. In Vitro **27,** 543–550
https://doi.org/10.1016/j.tiv.2012.09.023

Cai Q, Ma T, Li C, Tian Y, Li H (2016): Catalpol protects pre-myelinating oligodendrocytes against ischemia-induced oxidative injury through ERK1/2 signaling pathway. Int. J. Biol. Sci. **12,** 1415–1426
https://doi.org/10.7150/ijbs.16823

Chen Y, Zhang Y, Xu M, Luan J, Piao S, Chi S, Wang H (2017): Catalpol alleviates ovalbumin-induced asthma in mice: Reduced eosinophil infiltration in the lung. Int. Immunopharmacol. **43,** 140–146
https://doi.org/10.1016/j.intimp.2016.12.011

Cherry JD, Olschowka JA, O'Banion MK (2014): Neuroinflammation and M2 microglia: the good, the bad, and the inflamed. J. Neuroinflammation **11,** 98
https://doi.org/10.1186/1742-2094-11-98

Choi HJ, Jang HJ, Chung TW, Jeong SI, Cha J, Choi JY, Han CW, Jang YS, Joo M, Jeong HS, Ha KT (2013): Catalpol suppresses advanced glycation end-products-induced inflammatory responses through inhibition of reactive oxygen species in human monocytic THP-1 cells. Fitoterapia **86,** 19–28
https://doi.org/10.1016/j.fitote.2013.01.014

Choi HI, Choi JP, Seo J, Kim BJ, Rho M, Han JK, Kim JG (2017): Helicobacter pylori-derived extracellular vesicles increased in the gastric juices of gastric adenocarcinoma patients and induced inflammation mainly via specific targeting of gastric epithelial cells. Exp. Mol. Med. **49,** e330

https://doi.org/10.1038/emm.2017.47

Daulatzai MA (2016): Fundamental role of pan-inflammation and oxidative-nitrosative pathways in neuropathogenesis of Alzheimer's disease in focal cerebral ischemic rats. Am. J. Neurodegener. Dis. **5,** 102–130

Fan H, Wu PF, Zhang L, Hu ZL, Wang W, Guan XL, Luo H, Ni M, Yang JW, Li MX, Chen JG, Wang F (2015): Methionine sulfoxide reductase A negatively controls microglia-mediated neuroinflammation via inhibiting ROS/MAPKs/NF-κB signaling pathways through a catalytic antioxidant function. Antioxid. Redox Signal. **22,** 832–847

https://doi.org/10.1089/ars.2014.6022

Fetisova E, Chernyak B, Korshunova G, Muntyan M, Skulachev V (2017): Mitochondria-targeted antioxidants as a prospective therapeutic strategy for multiple sclerosis. Curr. Med. Chem. **24,** 2086–2114

https://doi.org/10.2174/0929867324666170316114452

Fu K, Piao T, Wang M, Zhang J, Jiang J, Wang X, Liu H (2014): Protective effect of catalpol on lipopolysaccharide-induced acute lung injury in mice. Int. Immunopharmacol. **23,** 400–406

https://doi.org/10.1016/j.intimp.2014.07.011

Garcia G, Nanni S, Figueira I, Ivanov I, McDougall GJ, Stewart D, Ferreira RB, Pinto P, Silva RF, Brites D, Santos CN (2017): Bioaccessible (poly)phenol metabolites from raspberry protect neural cells from oxidative stress and attenuate microglia activation. Food Chem. **215,** 274–283

https://doi.org/10.1016/j.foodchem.2016.07.128

Glass CK, Saijo K, Winner B, Marchetto MC, Gage FH (2010): Mechanisms underlying inflammation in neurodegeneration. Cell **140,** 918–934

https://doi.org/10.1016/j.cell.2010.02.016

Gomez-Nicola D, Perry VH (2015): Microglial dynamics and role in the healthy and diseased brain: a paradigm of functional plasticity. Neuroscientist **21,** 169–184

https://doi.org/10.1177/1073858414530512

Iizumi T, Takahashi S, Mashima K, Minami K, Izawa Y, Abe T, Hishiki T, Suematsu M, Kajimura M, Suzuki N (2016): A possible role of microglia-derived nitric oxide by lipopolysaccharide in activation of astroglial pentose-phosphate pathway via the Keap1/Nrf2 system. J. Neuroinflammation **13,** 99

https://doi.org/10.1186/s12974-016-0564-0

Jiang B, Du J, Liu JH, Bao YM, An LJ (2008): Catalpol attenuates the neurotoxicity induced by beta-amyloid(1-42) in cortical neuron-glia cultures. Brain Res. **1188,** 139–147

https://doi.org/10.1016/j.brainres.2007.07.105

Jin D, Cao M, Mu X, Yang G, Xue W, Huang Y, Chen H (2015): Catalpol inhibited the proliferation of T24 human bladder cancer cells by inducing apoptosis through the blockade of Akt-mediated anti-apoptotic signaling. Cell Biochem. Biophys. **71,** 1349–1356

https://doi.org/10.1007/s12013-014-0355-0

Kim YE, Hwang CJ, Lee HP, Kim CS, Son DJ, Ham YW, Hellström M, Han SB, Kim HS, Park EK, Hong JT (2017b): Inhibitory effect of punicalagin on lipopolysaccharide-induced neuroinflammation, oxidative stress and memory impairment via inhibition of nuclear factor-kappaB. Neuropharmacology **117,** 21–32

https://doi.org/10.1016/j.neuropharm.2017.01.025

Kopitar-Jerala N (2015): Innate immune response in brain, NF-Kappa B signaling and cystatins. Front. Mol. Neurosci. **8,** 73

https://doi.org/10.3389/fnmol.2015.00073

Lee IA, Hyam SR, Jang SE, Han MJ, Kim DH (2012): Ginsenoside Re ameliorates inflammation by inhibiting the binding of lipopolysaccharide to TLR4 on macrophages. J. Agric. Food Chem. **60,** 9595–9602

https://doi.org/10.1021/jf301372g

Lee MB, Lee JH, Hong SH, You JS, Nam ST, Kim HW, Park YH, Lee D, Min KY, Park YM, et al. (2017): JQ1, a BET inhibitor, controls TLR4-induced IL-10 production in regulatory B cells by BRD4-NF-κB axis. BMB Rep. **50,** 640–646

https://doi.org/10.5483/BMBRep.2017.50.12.194

Li Q, Verma IM (2002): NF-kappaB regulation in the immune system. Nat. Rev. Immunol. **2,** 725–734

https://doi.org/10.1038/nri910

Li X, Xu Z, Jiang Z, Sun L, Ji J, Miao J, Zhang X, Li X, Huang S, Wang T, Zhang L (2014): Hypoglycemic effect of catalpol on high-fat diet/streptozotocin-induced diabetic mice by increasing skeletal muscle mitochondrial biogenesis. Acta Biochim. Biophys. Sin. (Shanghai) **46,** 738–748

https://doi.org/10.1093/abbs/gmu065

Li Y, Bao Y, Jiang B, Wang Z, Liu Y, Zhang C, An L (2008): Catalpol protects primary cultured astrocytes from in vitro ischemia-induced damage. Int. J. Dev. Neurosci. **26,** 309–317

https://doi.org/10.1016/j.ijdevneu.2008.01.006

Liu C, Ma R, Wang L, Zhu R, Liu H, Guo Y, Zhao B, Zhao S, Tang J, Li Y, Niu J, Fu M, Zhang D, Gao S (2017a): Rehmanniae Radix in osteoporosis: A review of traditional Chinese medicinal uses, phytochemistry, pharmacokinetics and pharmacology. J. Ethnopharmacol. **198,** 351–362

https://doi.org/10.1016/j.jep.2017.01.021

Liu L, Gao H, Wang H, Zhang Y, Xu W, Lin S, Wang H, Wu Q, Guo J (2017b): Catalpol promotes cellular apoptosis in human HCT116 colorectal cancer cells via microRNA-200 and the downregulation of PI3K-Akt signaling pathway. Oncol. Lett. **14,** 3741–3747

https://doi.org/10.3892/ol.2017.6580

Matsumoto Y, Sekimizu K (2016): A hyperglycemic silkworm model for evaluating hypoglycemic activity of Rehmanniae Radix, an herbal medicine. Drug Discov. Ther. **10,** 14–18

https://doi.org/10.5582/ddt.2016.01016

Ohl K, Tenbrock K, Kipp M (2016): Oxidative stress in multiple sclerosis: Central and peripheral mode of action. Exp. Neurol. **277,** 58–67

https://doi.org/10.1016/j.expneurol.2015.11.010

Park YS, Kwon YJ, Chun YJ (2017): CYP1B1 Activates Wnt/β-catenin signaling through suppression of Herc5-mediated ISGylation for protein degradation on β-catenin in HeLa cells. Toxicol. Res. **33,** 211–218

https://doi.org/10.5487/TR.2017.33.3.211

Slusarczyk J, Trojan E, Glombik K, Piotrowska A, Budziszewska B, Kubera M, Popiolek-Barczyk K, Lason W, Mika J, Basta-Kaim A (2016): Anti-inflammatory properties of tianeptine on lipopolysaccharide-induced changes in microglial cells involve toll-like receptor-related pathways. J. Neurochem. **136,** 958–970

https://doi.org/10.1111/jnc.13452

Tian YY, An LJ, Jiang L, Duan YL, Chen J, Jiang B (2006): Catalpol protects dopaminergic neurons from LPS-induced neurotoxicity in mesencephalic neuron-glia cultures. Life Sci. **80,** 193–199
https://doi.org/10.1016/j.lfs.2006.09.010

Tremblay MÈ, Stevens B, Sierra A, Wake H, Bessis A, Nimmerjahn A (2011): The role of microglia in the healthy brain. J. Neurosci. **31,** 16064–16069
https://doi.org/10.1523/JNEUROSCI.4158-11.2011

von Bernhardi R, Eugenín-von Bernhardi L, Eugenín J (2015): Microglial cell dysregulation in brain aging and neurodegeneration. Front. Aging Neurosci. **7,** 124
https://doi.org/10.3389/fnagi.2015.00124

Wang X, Wang C, Wang J, Zhao S, Zhang K, Wang J, Zhang W, Wu C, Yang J (2014): Pseudoginsenoside-F11 (PF11) exerts anti-neuroinflammatory effects on LPS-activated microglial cells by inhibiting TLR4-mediated TAK1/IKK/NF-κB, MAPKs and Akt signaling pathways. Neuropharmacology **79,** 642–656
https://doi.org/10.1016/j.neuropharm.2014.01.022

Wang ZH, Zhan-Sheng H (2018): Catalpol inhibits migration and induces apoptosis in gastric cancer cells and in athymic nude mice. Biomed. Pharmacother. **103,** 1708–1719
https://doi.org/10.1016/j.biopha.2018.03.094

Xiao WQ, Yin GJ, Fan YT, Qiu L, Cang XF, Yu G, Hu YL, Xing M, Wu DQ, Wang XP, Hu GY, Wan R (2014): Catalpol ameliorates sodium taurocholate-induced acute pancreatitis in rats via inhibiting activation of nuclear factor kappa B. Int. J. Mol. Sci. **15,** 11957–11972
https://doi.org/10.3390/ijms150711957

Zeng KW, Zhao MB, Ma ZZ, Jiang Y, Tu PF (2012): Protosappanin A inhibits oxidative and nitrative stress via interfering the interaction of transmembrane protein CD14 with Toll-like receptor-4 in lipopolysaccharide-induced BV-2 microglia. Int. Immunopharmacol. **14,** 558–569
https://doi.org/10.1016/j.intimp.2012.09.004

Zhang XL, Jiang B, Li ZB, Hao S, An LJ (2007): Catalpol ameliorates cognition deficits and attenuates oxidative damage in the brain of senescent mice induced by D-galactose. Pharmacol. Biochem. Behav. **88,** 64–72
https://doi.org/10.1016/j.pbb.2007.07.004

Zhang RX, Li MX, Jia ZP (2008): Rehmannia glutinosa: review of botany, chemistry and pharmacology. J. Ethnopharmacol. **117,** 199–214
https://doi.org/10.1016/j.jep.2008.02.018

Zhang A, Hao S, Bi J, Bao Y, Zhang X, An L, Jiang B (2009): Effects of catalpol on mitochondrial function and working memory in mice after lipopolysaccharide-induced acute systemic inflammation. Exp. Toxicol. Pathol. **61,** 461–469
https://doi.org/10.1016/j.etp.2008.10.010

Zhang YP, Pan CS, Yan L, Liu YY, Hu BH, Chang X, Li Q, Huang DD, Sun HY, Fu G, Sun K, Fan JY, Han JY (2016): Catalpol restores LPS-elicited rat microcirculation disorder by regulation of a network of signaling involving inhibition of TLR-4 and SRC. Am. J. Physiol. Gastrointest. Liver Physiol. **311,** G1091–G1104
https://doi.org/10.1152/ajpgi.00159.2016

Zhang H, Jia R, Wang F, Qiu G, Qiao P, Xu X, Wu D (2017): Catalpol protects mice against lipopolysaccharide/D-galactosamine-induced acute liver injury through inhibiting inflammatory and oxidative response. Oncotarget **9,** 3887–3894

Zheng XW, Yang WT, Chen S, Xu QQ, Shan CS, Zheng GQ, Ruan JC (2017): Neuroprotection of catalpol for experimental acute focal ischemic stroke: Preclinical evidence and possible mechanisms of antioxidation, anti-Inflammation, and antiapoptosis. Oxid. Med. Cell Longev. **2017,** 5058609
https://doi.org/10.1155/2017/5058609

Zhou J, Xu G, Ma S, Li F, Yuan M, Xu H, Huang K (2015): Catalpol ameliorates high-fat diet-induced insulin resistance and adipose tissue inflammation by suppressing the JNK and NF-κB pathways. Biochem. Biophys. Res. Commun. **467,** 853–858
https://doi.org/10.1016/j.bbrc.2015.10.054

Zhu H, Wang Y, Liu Z, Wang J, Wan D, Feng S, Yang X, Wang T (2016): Antidiabetic and antioxidant effects of catalpol extracted from Rehmannia glutinosa (Di Huang) on rat diabetes induced by streptozotocin and high-fat, high-sugar feed. Chin. Med. **11,** 25
https://doi.org/10.1186/s13020-016-0096-7